

PAPER • OPEN ACCESS

Dielectric Analysis of Amine Modified Nano-graphite: Effects of Thickness, Temperature and Frequency

To cite this article: Bhanu Pratap Singh *et al* 2024 *IOP Conf. Ser.: Mater. Sci. Eng.* **1300** 012011

View the [article online](#) for updates and enhancements.

You may also like

- NiO/nanoporous graphene composites with excellent supercapacitive performance produced by atomic layer deposition
Caiying Chen, Chaoqu Chen, Peipei Huang *et al*
- Performance Evaluation of an Anode-Supported QDSC Short-Stack Operating with Different Fuel Mixtures in Stationary QDSC System
Francesco Marino, Andrea Monforti Ferrario, Francesca Santoni *et al*
- N-doped graphene encapsulated MoS₂ nanosphere composite as a high-performance anode for lithium-ion batteries
Yating Zhang, Zhanrui Zhang, Youyu Zhu *et al*

PAPER INFORMATION

ARTICLE ID: 1300012011

ISSN: 1755-1315

DOI: 10.1088/1755-1315/1300/1/012011

URL: [http://iopscience.iop.org/1755-1315/1300/1/012011](#)

PDF: [http://iopscience.iop.org/1755-1315/1300/1/012011/pdf/1300012011.pdf](#)

XML: [http://iopscience.iop.org/1755-1315/1300/1/012011/xml](#)

HTML: [http://iopscience.iop.org/1755-1315/1300/1/012011/html](#)

EPUB: [http://iopscience.iop.org/1755-1315/1300/1/012011/epub](#)

PDF: [http://iopscience.iop.org/1755-1315/1300/1/012011/pdf/1300012011.pdf](#)

XML: [http://iopscience.iop.org/1755-1315/1300/1/012011/xml](#)

HTML: [http://iopscience.iop.org/1755-1315/1300/1/012011/html](#)

EPUB: [http://iopscience.iop.org/1755-1315/1300/1/012011/epub](#)

PDF: [http://iopscience.iop.org/1755-1315/1300/1/012011/pdf/1300012011.pdf](#)

XML: [http://iopscience.iop.org/1755-1315/1300/1/012011/xml](#)

HTML: [http://iopscience.iop.org/1755-1315/1300/1/012011/html](#)

EPUB: [http://iopscience.iop.org/1755-1315/1300/1/012011/epub](#)

PDF: [http://iopscience.iop.org/1755-1315/1300/1/012011/pdf/1300012011.pdf](#)

XML: [http://iopscience.iop.org/1755-1315/1300/1/012011/xml](#)

HTML: [http://iopscience.iop.org/1755-1315/1300/1/012011/html](#)

EPUB: [http://iopscience.iop.org/1755-1315/1300/1/012011/epub](#)

PDF: [http://iopscience.iop.org/1755-1315/1300/1/012011/pdf/1300012011.pdf](#)

XML: [http://iopscience.iop.org/1755-1315/1300/1/012011/xml](#)

HTML: [http://iopscience.iop.org/1755-1315/1300/1/012011/html](#)

EPUB: [http://iopscience.iop.org/1755-1315/1300/1/012011/epub](#)

PDF: [http://iopscience.iop.org/1755-1315/1300/1/012011/pdf/1300012011.pdf](#)

XML: [http://iopscience.iop.org/1755-1315/1300/1/012011/xml](#)

HTML: [http://iopscience.iop.org/1755-1315/1300/1/012011/html](#)

EPUB: [http://iopscience.iop.org/1755-1315/1300/1/012011/epub](#)

PDF: [http://iopscience.iop.org/1755-1315/1300/1/012011/pdf/1300012011.pdf](#)

XML: [http://iopscience.iop.org/1755-1315/1300/1/012011/xml](#)



ECS UNITED

ECS The Electrochemical Society
Advancing solid state & electrochemical science & technology

247th ECS Meeting
Montréal, Canada
May 18-22, 2025
Palais des Congrès de Montréal

Showcase your science!

Abstracts due December 6th

Dielectric Analysis of Amine Modified Nano-graphite: Effects of Thickness, Temperature and Frequency

Bhanu Pratap Singh¹, Pushpendra Kumar² and S. P. Mahapatra^{1*}

¹Department of Chemistry, National Institute of Technology Raipur 492010 India

²Department of Chemistry, Guru Ghasidas Vishwavidyalaya, Bilaspur 497101 India

*Corresponding Author: spmahapatra.chy@nitrr.ac.in

Keywords:
Frequency

Abstract. Amine modified nano-graphite (NH₂-NG) has been produced from nano-graphite (NG) powder via liquor ammonia (NH₃) aqueous solution by microwave, ultrasonic methods. The surface modified NG have been characterized by X-ray diffraction (XRD), scanning electron microscopy (SEM) and Fourier-transform infrared spectroscopy (FTIR) techniques which clearly demonstrate that synthesis of NH₂-NG was successful. The crystalline characteristics of amine modified nano-graphite powder have been studied through XRD technique. The morphology structure of synthesized surface modified nanoparticles has been determined by SEM analysis. FTIR spectra confirmed the existence of amine groups on the surface of produced nano-graphite powder. NH₂-NG pellet was prepared to analyse its dielectric properties as a function of thickness (1, 2, 3, 5 and 7 mm), frequency (range 10⁻²-10⁵ Hz) and temperature (25, 50, 75 and 100 °C). As a function of frequency, the dielectric loss tangent and permittivity each exhibit a distinct relaxation peak that grows up to a thickness of 5 mm then decreasing. Because nanoparticles are capacitive, the capacitance values of NG and NH₂-NG increase with thicknesses up to 5 mm and drop with frequency. The drop in dielectric permittivity of NG and NH₂-NG pellets after 5 mm may be caused by an increase in resistivity. Positive temperature coefficient (PTC) of increased conductance is confirmed by the continuous increase in electrical conductivity of NG and NH₂-NG with temperature. The degree of temperature has a significant impact on the dielectric loss tangent, dielectric permittivity, and electrical conductivity of NG, and NH₂-NG.

1. Introduction

Different method has been reported for the surface modification of graphite oxide powder. Among them, introduction of surface modification of graphite oxide via reductive modification is considered as one of the most effective routes. In the literature, several reducing agents have been employed including ammonia solution (25 wt% in water) by one-pot solvothermal process [1], Graphite with an -NH₂ group was created using vacuum ultraviolet-induced photochemistry when ammonia was present [2]. However, due to their instrumental setup, some of the aforementioned approaches are costly and necessitate significant attention because multiple sensitive parameters must be maintained during the functionalization process. For this reason, it is thought that a straightforward wet chemical method offers a practical, affordable, and easy way to directly attach the -NH₂ group to the surface of nano-graphite. No such procedure has, as far as we are aware, been documented. Hydrazine-induced reduction of graphite and graphene oxides [3] Graphene oxide (GO) sheets, the layered structure of graphite oxide, are decorated on their basal planes and edges with a variety of oxygen functional



Content from this work may be used under the terms of the Creative Commons Attribution 3.0 licence. Any further distribution of this work must maintain attribution to the author(s) and the title of the work, journal citation and DOI.

groups, which significantly alter the van der Waals interactions between the layers and give GO its strong hydrophilicity. Thus, Surface modification of graphite oxide by hydrazine reduction [4] by simple ultrasonication and stirring. By adding improved NG to different kinds of polymers and other materials, composite materials can have their conductivity, tensile strength, and elasticity increased. They can be used as the conductor substantial for batteries, capacitors, double-layer capacitors, and improved microelectronic devices [5-8]. Capacitors use dielectric materials with low losses and high permittivity to store more electrical energy [9, 10]. Graphite is a well-known type of carbon that has a planar and layered structure. Because of its exceptional optical, thermal, electrical, and power properties as well as its distinct two-dimensional structure, graphene is now a viable substitute for many different applications, including photovoltaic, catalysis, nano-electronic, and energy conversion and storage [11-13]. Dielectric materials are used in the fabrication of microelectronics for large-scale power applications and energy storage devices [14]. Lyddane-Sachs-Teller states that lattice vibrations create a shift in the intrinsic dipole moment, which increases the permittivity to a very high value [15]. There aren't many studies on graphene oxide or graphene-based material composites' dielectric analysis in the literature [16, 17]. According to Verdejo et al.'s research, graphene oxide can be uniformly distributed throughout the polymer cross-section to achieve a satisfactory increase in dielectric permittivity [18]. The earliest techniques to synthesise graphene nanosheets from bulk graphite were the scotch-tape technique and epitaxial chemical vapours deposition [19, 20]. In the current work, graphite powder was used to create NG powder, and an aqueous liquid ammonia (NH_3) solution was used to modify the powder's surface. The morphological structure of NG and NH_2 -NG was examined using SEM and XRD analysis. With the use of FTIR spectroscopy, the amine group of altered NG was identified. For use in various sectors, the dielectric relaxation spectra (DRS) of NG and NH_2 -NG pellets was investigated. Capacitance, dielectric permittivity, dielectric loss tangent and electrical conductivity measurements were among the tasks included in this.

2. Experimental

2.1 Compounds

Graphite powder (size < 20 μm), liquor NH_3 (98%).

2.2 Preparation of nano-graphite

Synthesis of nano-graphite by graphite powder already discuss to our previous paper [21].

2.3 preparation of amine modified nano-graphite

A quantity of 2 gm of prepared nano graphite was reduced by liquor ammonia aqueous solution (20 ml liquor NH_3 , 80 ml distilled water), accompanied by ultrasonic treatment for more than 24 h and then filtered many times and dried to 80 $^\circ\text{C}$ at 24 h. The resultant amine modified nano graphite. powder was finally dried in a vacuum oven at 120 $^\circ\text{C}$.

3. Measurements

3.1 Characterization Techniques

Using a SEM (ZEISS EVO-50, Germany), the morphological properties of the synthesised NG and NH_2 -NG powder were investigated. FTIR spectroscopy (Bruker Scientific Instrument, US) was used to analyse the amine groups in modified NG. X-ray diffraction (XPert Pro PANalytical, Netherlands) was used to confirm the crystal structures of the generated NG and NH_2 -NG. In the 10-2-105 Hz frequency range, the dielectric characteristics of NG and NH_2 -NG pellets were examined using the Hi-Tester LCR metre, Hioki 3533. Based on measurements of the dielectric, the following relationship has been used to evaluate electrical conductivity:

$$\sigma_{AC} = \omega \epsilon^0 \epsilon' \tan \delta \quad (1)$$

Where, $\omega = 2\pi f$ (f is frequency), ϵ' = dielectric constant (C_p/C_0), ϵ^0 = vacuum permittivity and $\tan \delta$ = dielectric loss tangent [22].

4. Results and Discussion

4.1 Scanning Electron Microscopy

SEM operating at 8.5 mm and 20 kV in high vacuum mode was used to examine the morphology of prepared NG and NH_2 -NG. Figure 1(a) and (b) display SEM images of NG and NH_2 -NG. As can be seen from Figure 1(a), NG has a smooth surface and a crumpled shrill sheet structure, whereas Figure

1(b) displays a wrinkled and rough surface because $\text{NH}_2\text{-NG}$'s surface contains amine groups.



Figure 1 SEM image of (a) NG (b) $\text{NH}_2\text{-NG}$.

4.2 X-Ray Diffraction

Using the XRD method, the crystal structures of produced NG and $\text{NH}_2\text{-NG}$ were identified. Figure 2 shown the XRD spectra of produced NG and $\text{NH}_2\text{-NG}$. NG and $\text{NH}_2\text{-NG}$ display 2θ at 26.46° and FWHM of 1.9441 with 0.12 nm d-spacing [23]. NG and $\text{NH}_2\text{-NG}$ have a crystalline size of 4.34 nm according to the Scherer and Bragg equations [24]. There are no structural changes, but the peaks have widened and become less intense, indicating a decrease in particle size.

$$D_p = (0.94 \times \lambda) / (\beta \times \cos\theta)$$

Where, D_p is Average Crystallite size and β is Line broadening in radians,

Bragg's equation:

$$n\lambda = 2d\sin\theta$$

Where, n is Diffraction series, λ is X-Ray wavelength, d is Interlayer spacing and θ is Bragg angle,

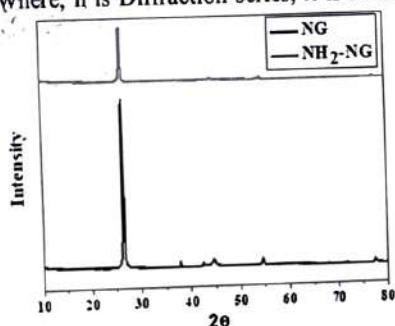


Figure 2 XRD of NG and $\text{NH}_2\text{-NG}$.

4.3 Fourier-Transform Infrared Spectroscopy

Using FTIR spectroscopy, the various functional groups of amines that changed NG were examined. Figure 3 shown the FTIR data of $\text{NH}_2\text{-NG}$. The results demonstrated that whereas NG exhibits no absorption peaks, $\text{NH}_2\text{-NG}$ has those that are associated with particular functional groups. A portion of the absorption peaks at 3390.31 cm^{-1} are caused by the N-H stretching vibration. The FTIR spectrum of $\text{NH}_2\text{-NG}$ demonstrates the effective amine modification of graphite powder. The C=C stretching vibration is attributed to the peak at 1625.57 cm^{-1} , whereas two new nitrogen-related peaks at 1019.18 cm^{-1} and 1619.56 cm^{-1} were seen. The amide's C-N stretching and N-H bending bonds can be roughly attributed to these peaks, respectively.

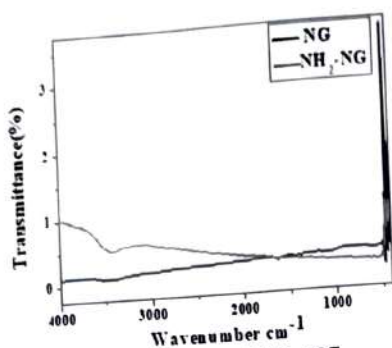


Figure 3 FTIR of NG and NH₂-NG

4.4 Dielectric Loss Tangent ($\tan \delta$)

The $\tan \delta$ of synthesised NG and NH₂-NG has been calculated with frequency at different thicknesses (1 to 7 mm) at 25°C temperature and different temperatures (25°C, 50°C, 75°C, and 100°C) at 3mm thickness is shown in Figure 4 (a) and (b) Figure 5 (a) and (b) respectively. The $\tan \delta$ rises with frequency at all thicknesses and temperatures of NG and NH₂-NG pellets; however, this rise does not continue after reaching a peak; rather, it decreases with frequency because polar groups are present in the prepared NH₂-NG. Additionally, it is noted that when amine functional groups are present, the peak of NH₂-NG shifts. The primary determinant of the relaxation behaviour of NG and NH₂-NG pellets at room temperature is their thickness. The maximum $\tan \delta$ rises with NG and NH₂-NG pellet thickness up to 5 mm; this may be because of charge conduction and dipole relaxation that has occurred [25] and reductions for a thickness of 7 mm, which may be because of resistivity and dipole fluctuation that is increasing within NG and NH₂-NG pellets [26]. As temperature rises (Figure 5(a)), the maximum $\tan \delta$ value increases towards lower to higher frequency; but, when temperature rises (Figure 5(b)), the maximum $\tan \delta$ value increases towards higher to lower frequency. Temperature affects how frequently this maximum dielectric loss tangent manifests.

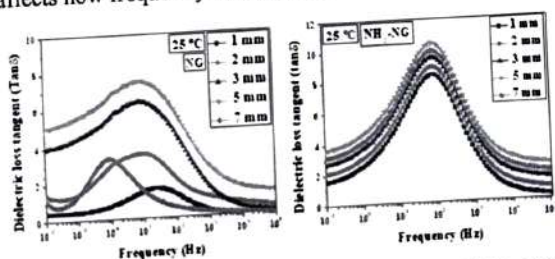


Figure 4 Dielectric loss tangent of (a) NG and (b) NH₂-NG effect of thickness.

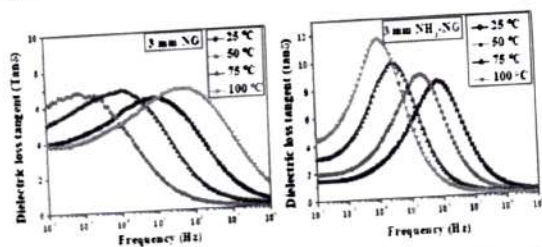


Figure 5 Dielectric loss tangent of (a) NG and (b) NH₂-NG effect of temperature.

4.5 Dielectric Permittivity (ϵ')

The ϵ' of a substance indicates the level of electrical polarisation. Synthesised NG and NH₂-NG nanoparticle thickness variations with frequency at 1, 2, 3, 5, and 7 mm are depicted in Figure 6(a) and (b) at room temperature and at various temperatures (25, 50, 75, and 100 °C) in Figure 7(a) and (b). The dielectric permittivity of modified NG grows with thickness and decreases with frequency as a

result of the functional groups' ionic convergence and transmitting aerial change [27]. The graphic illustrates how the thickness of the NG and NH₂-NG pellets causes a rise in dielectric permittivity. The highly conductive character of the NG and NH₂-NG nanoparticles, as well as the positive temperature coefficient (PTC) impact [28], are the reasons behind the observation that dielectric permittivity rises with temperature (Figure 7(a) and (b)). The high electrical conductivity of NG and NH₂-NG and the ferroelectric character of the conductive particles may be the cause of the greater dielectric permittivity at low frequencies [29, 30].

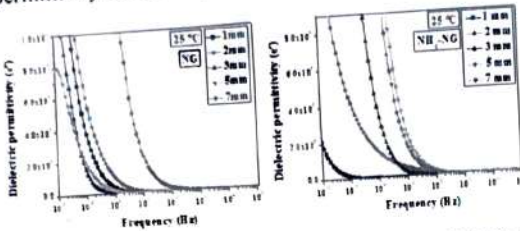


Figure 6 Dielectric permittivity of (a) NG and (b) NH₂-NG effect of thickness.

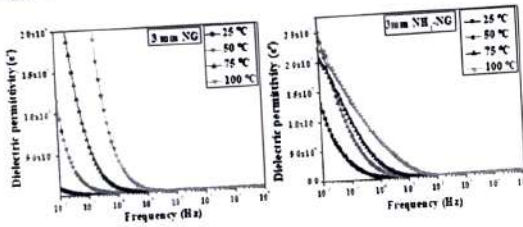


Figure 7 Dielectric permittivity of (a) NG and (b) NH₂-NG effect of temperature.

4.6 Electrical Conductivity (σ)

Electrical conductivity is the ability to carry electrical current. Figures 8(a) and (b) illustrate how the σ of NG and NH₂-NG pellets varies with frequency at various thicknesses. Both the thickness of NG and NH₂-NG pellets and their frequency cause a constant rise in σ . The image illustrates how the thickness of NG and NH₂-NG pellets up to 5 mm increases σ due to nanoparticle impacts creating a continuous conduit for electrons to traverse across the volume of the sample. The reduction in σ at a thickness of 7 mm could be attributed to the creation of agglomerates of nanoparticles and the deformation of continuous paths. Additionally, a drop in the dielectric permittivity and loss tangent may be the cause of the electrical conductivity decline [31]. It is also observed that σ of NG and NH₂-NG increases continuously with increasing temperature (Figure 9 (a) and (b)). This validates the greater conductance PTC effect. The curve displays both a DC and AC conductivity region up to 50 °C, but as temperature rises, it only displays AC conductivity. Thermal activation of charge carriers results in an increase in AC conductivity, and this rise in electrical conductivity with temperature is typically the result of the net effect [32].

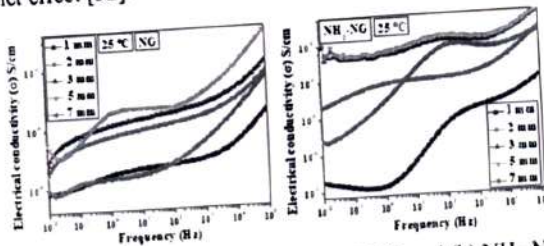


Figure 8 Electrical Conductivity of (a) NG and (b) NH₂-NG effect of thickness.

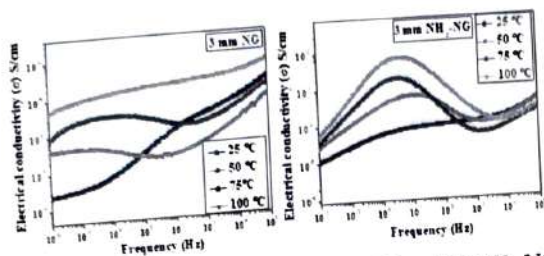


Figure 9 Electrical Conductivity of (a) NG and (b) NH₂-NG effect of temperature.

4.7 Percolation Behaviour

The percolation behaviour of the σ of NG and NH₂-NG pellets with thickness at various frequencies (1 to 100 kHz) is shown to vary in Figures 10(a) and (b). The σ of the NG and NH₂-NG pellets grows exponentially to a thickness of 5 mm, after which it decreases to a thickness of 7 mm. The agglomeration of nanoparticles may be the cause of this [33]. As shown in Figures 11(a) and (b), the σ of NG and NH₂-NG pellets can be divided into three zones. The first zone is inductive; electrical conductivity progressively increases with thickness as charge nanoparticle density falls. The third zone, known as the saturation region, is when the agglomerate's production of NG and NH₂-NG nanoparticles results in either a minor increase in σ or a decrease in it. The constant development of conductive paths results in a dramatic increase in σ in the second region, known as the percolation region. The percolation thresholds for NG and NH₂-NG pellets have been found to vary in thickness from 4 to 5 mm.

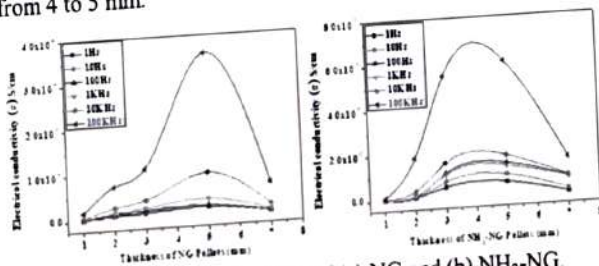


Figure 10 Percolation behaviour of (a) NG and (b) NH₂-NG.

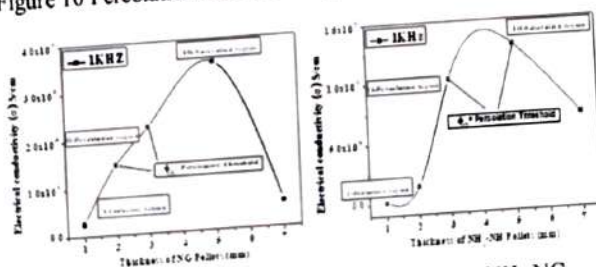


Figure 11 Electrical conductivity of (a) NG and (b) NH₂-NG.

5. Conclusions

Graphite powder was successfully converted into nano-graphite and amine modified nanoparticles using the oxidation process. The surface morphology of NG and NH₂-NG is confirmed by SEM pictures. The existence of amine groups on the surface of the manufactured NG powder was verified by FTIR measurements. The interlayer spacing of 0.12 nm is indicated by 2θ at 26.46° in the XRD data of NG and NH₂-NG. The inclusion of ionic groups in the modified NH₂-NG causes peak shifts and relaxation peaks with frequency in the $\tan \delta$ spectra. Dielectric permittivity increases with thickness and temperature and decreases with frequency; these changes may be caused by the functional groups of modified NH₂-NG's charge orientation and dipole moment modification. Because

conducting nanoparticles are ferroelectric, they have a larger dielectric permittivity at low frequencies. The thickness and temperature of NG and NH₂-NG pellets, along with frequency, all contribute to the ongoing rise in σ . The σ rises with NG and NH₂-NG particle thickness up to 5 mm, after which its reductions to 7 mm. This could be because the loss tangent and dielectric permittivity are decreasing. It has been determined that the percolation thresholds of NG and NH₂-NG pellets fall between 4-5 mm thicknesses. These findings show that NG and NH₂-NG nanoparticles have tremendous potential for use in energy storage devices, sensors, and electrical applications based on high dielectric.

Acknowledgements

The directors of the National Institute of Technology in Raipur are appreciated by the authors for their facilities and assistance.

References

- [1] Zhang C, Hao R, Liao H and Hou Y 2013 *Nano Energy*. Jan 2 88
- [2] Girard-Lauriault PL, Illgen R, Ruiz JC, Wertheimer MR and Unger WE 2012 *Appl. Surf. Sci.* **258** 8448
- [3] Park S, An J, Potts JR, Velamakanni A, Murali S and Ruoff RS 2011 *carbon*. **49** 3019
- [4] Ren PG, Yan DX, Ji X, Chen T and Li ZM 2010 *Nanotechnology*. **22** 055705
- [5] Dou L, Cui F, Yu Y, Khanarian G, Eaton SW, Yang Q, Resasco J, Schildknecht C, Schierle-Arndt K and Yang P 2016 *Acs Nano*. **10** 2600
- [6] Hsu T, Epting WK, Mahub R, Nuhfer NT, Bhattacharya S, Lei Y, Miller HM, Ohodnicki PR, Gerdes KR, Abernathy HW and Hackett GA 2018 *J. Power Sources*. **386** 1
- [7] Schönhals A and Kremer F 2003 Analysis of dielectric spectra. In Broadband dielectric spectroscopy 59 Berlin, Heidelberg: Springer Berlin Heidelberg.
- [8] Kumar P, Penta S and Mahapatra SP 2019 *Integr. Ferroelectr.* **202** 41
- [9] Wu Y, Wang Z, Shen X, Liu X, Han NM, Zheng Q, Mai YW and Kim JK 2018 *ACS Appl. Mater. Interfaces*. **10** 26641
- [10] Homes CC and Vogt T 2013 *Nat. Mater.* **12** 782
- [11] Hao X 2013 *J. Adv. Dielectr.* **3** 1330001
- [12] He L, Neaton JB, Cohen MH, Vanderbilt D and Homes CC 2002 *Phys. Rev. B*. **65** 214112
- [13] Gao Y and Hao P 2009 *Physica E Low Dimens. Syst. Nanostruct.* **41** 1561
- [14] Berger C, Song Z, Li X, Wu X, Brown N, Naud C, Mayou D, Li T, Hass J, Marchenkov AN and Conrad EH 2006 *Science*. **312** 1191
- [15] Stankovich S, Dikin DA, Dommett GH, Kohlhaas KM, Zimney EJ, Stach EA, Piner RD, Nguyen ST and Ruoff RS 2006 *nature*. **442** 282
- [16] De Wild J, Meijerink A, Rath JK, Van Sark WG and Schropp RE 2011 *Energy Environ. Sci.* **4** 4835
- [17] Liu Y, Dong X and Chen P 2012 *Chem. Soc. Rev.* **41** 2283
- [18] Hu W, Liu Y, Withers RL, Frankcombe TJ, Norén L, Snashall A, Kitchin M, Smith P, Gong B, Chen H and Schiemer J 2013 *Nat. Mater.* **12** 821
- [19] Ramanathan T, Abdala AA, Stankovich S, Dikin DA, Herrera-Alonso M, Piner RD, Adamson DH, Schniepp HC, Chen XR, Ruoff RS and Nguyen ST 2008 *Nat. Nanotechnol.* **3** 327
- [20] Dikin DA, Stankovich S, Zimney EJ, Piner RD, Dommett GH, Evmenenko G, Nguyen ST and Ruoff RS 2007 *Nature*. **448** 457
- [21] Singh BP, Kumar P and Mahapatra SP, 2023 *Ferroelectrics*. **51** 617
- [22] Kremer F and Schönhals A 2002 editors. Broadband dielectric spectroscopy. Springer Science & Business Media
- [23] Shalaby A, Nihtianova D, Markov P, Staneva AD, Iordanova RS and Dimitriev YB 2015 *Bulg. Chem. Commun.* **47** 291
- [24] Li J, Zeng X, Ren T and Van der Heide E 2014 *Lubricants*. **2** 137
- [25] Sebastian MT, Silva MA and Sombra AS 2017 *Microwave materials and applications 2V set*. **5** 1
- [26] Kumar P, Penta S and Mahapatra SP 2020 *J. Electron. Mater.* **49** 5801
- [27] Tiwari SK, Choudhary RN and Mahapatra SP 2015 *High Perform. Polym.* **27** 274
- [28] Saji J, Khare A and Mahapatra SP 2015 *Fibers Polym.* **16** 883

- [29] Pastor M, Bajpai PK and Choudhary RN 2007 *J. Phys. Chem. Solids.* **68** 1914
- [30] Kurchak AI, Eliseev EA, Kalinin SV, Strikha MV and Morozovska AN 2017 *Phys. Rev. Appl.* **8** 024027
- [31] Das PS, Chakraborty PK, Behera B and Choudhary RN 2007 *Phys. B: Condens. Matter.* **395** 98
- [32] Panda S, Goswami S and Acharya B 2019 *J. Electron. Mater.* **48** 2853
- [33] Xu D, Sridhar V, Mahapatra SP and Kim JK 2009 *J. Appl. Polym. Sci.* **111** 1358